ARMY RESEARCH LABORATORY

Numerical Simulation of the Flow in a 1:57-Scale Axisymmetric Model of a Large Blast Simulator

Klaus O. Opalka

ARL-TR-111   April 1993

NOTICES

Destroy this report when it is no longer needed. DO NOT return it to the originator.

The findings of this report are not to be construed as an official Department of the Army position, unless so designated by other authorized documents.

The use of trade names or manufacturers' names in this report does not constitute indorsement of any commercial product.

1. AGENCY USE ONLY (Leave blank)	2. REPORT DATE April 1993	3. REPORT TYPE AND DATES COVERED Final, 15 January–31 December 1992

4. TITLE AND SUBTITLE	5. FUNDING NUMBERS
Numerical Simulation of the Flow in a 1:57-Scale Axisymmetric Model of a Large Blast Simulator	WO: 44061-203-63-0001

6. AUTHOR(S)

Klaus O. Opalka

7. PERFORMING ORGANIZATION NAME(S) AND ADDRESS(ES)	8. PERFORMING ORGANIZATION REPORT NUMBER
U.S. Army Research Laboratory ATTN: AMSRL-WT-NC Aberdeen Proving Ground, MD 21005-5066	

9. SPONSORING/MONITORING AGENCY NAME(S) AND ADDRESS(ES)	10. SPONSORING/MONITORING AGENCY REPORT NUMBER
U.S. Army Research Laboratory ATTN: AMSRL-OP-CI-B (Tech Lib) Aberdeen Proving Ground, MD 21005-5066	ARL-TR-111

11. SUPPLEMENTARY NOTES

12a. DISTRIBUTION/AVAILABILITY STATEMENT	12b. DISTRIBUTION CODE
Approved for public release; distribution is unlimited.	

13. ABSTRACT (Maximum 200 words)

This report presents an assessment of the suitability of the USA-RG2 hydrocode for simulating the flow in a variable-area shock tunnel. A multi-zone gridding technique is used to model the 1:57-Scale LBS test facility at the U.S. Army Research Laboratory. Computations for various grid configurations employing inviscid and viscous solution algorithms and three turbulence models were executed and the results are compared to experimental data. The need for an adequate mesh density in the grid to obtain a realistic flow simulation and the advantage of solving the full Navier-Stokes equations with added k-ε turbulence model for the experiment chosen as a bench mark are demonstrated.

14. SUBJECT TERMS	15. NUMBER OF PAGES
gas dynamics, unsteady flow, computer applications, fluid dynamics, blast waves, inviscid flow, computational fluid dynamics, blast-wave simulation, axisymmetric flow, computer aided design, shock tubes, viscous flow, turbulence	31
	16. PRICE CODE

17. SECURITY CLASSIFICATION OF REPORT	18. SECURITY CLASSIFICATION OF THIS PAGE	19. SECURITY CLASSIFICATION OF ABSTRACT	20. LIMITATION OF ABSTRACT
UNCLASSIFIED	UNCLASSIFIED	UNCLASSIFIED	SAR

Contents

Figures

Tables

Acknowledgment

1. Introduction

The Blast/Thermal Effects (BTE) Branch in the U.S. Army Research Laboratory (ARL), formerly a branch in the U.S. Army Ballistic Research Laboratory (BRL), is involved in the design and construction of a Large Blast/Thermal Simulator (LB/TS) as a consultant to the Defense Nuclear Agency (DNA). A LB/TS is an experimental facility for the simulation of decaying blast waves such as are encountered in nuclear explosions. Blast and thermal effects can be simulated in this laboratory environment without generating nuclear radiation. The facility will be equipped with nine blast generator tubes which discharge high-pressure, high-temperature nitrogen into a large tunnel. The expanding gas generates the decaying blast wave. A Rarefaction Wave Eliminator (RWE) located at the open end of the tunnel will prevent wave reflections of the exiting flow which would travel back into the tunnel destroying the flow simulation. This is effected by opening and closing, in a prescribed fashion, a large array of louvers which controls the exit flow area.

It is necessary to obtain an accurate prediction of the experimental blast wave, in order to calculate an opening and closing function which can be fed to the RWE controller during the test preparation phase. For this purpose, various hydrodynamic computer codes are being investigated and evaluated for their applicability to the present problem. One of these codes is the Unified Solution Algorithm for Real Gas in Two Dimensions (USA-RG2) code developed at the Rockwell International Science Center (RISC). This code was made available to the BTE branch in ARL under a consultative agreement for solving particular problems, one of which is reported here, and involves the flow simulation in an axisymmetric shock tunnel. Various flow computations, inviscid and viscous, using three different turbulence models, and based on several grid variations are executed. The results are presented and compared with experimental data.

2. The U.S. LB/TS Development

For simulating ideal blast waves, the U.S. Army and DNA have proposed the construction of a test facility large enough to test full-sized military equipment in order to meet the growing need for blast and thermal survivability testing and to conduct research into nuclear blast phenomenology. In 1982, BRL was chosen as the lead laboratory for the research and development effort of this project, and has developed a concept of such a LB/TS facility over the past ten years (Mark et al. 1983; Pearson et al. 1985,1987; Opalka and Pearson 1988,1989). The proposed U.S. LB/TS is suitable to simulate both thermal and blast effects of nuclear explosions over a wide variety of shock overpressures (2-35 psi) and weapon yields (1-600 kT) without generating nuclear radiation effects.

In 1988, DNA assumed responsibility for the design of this facility (Figure 1a), and its construction is to be executed by the Corps of Engineers. The White Sands Missile Range, New Mexico, was chosen for its location. The BTE branch of ARL was retained by DNA as consultant for this project.

An LB/TS is basically a shock tunnel with a variable cross-sectional area along its length. It serves to simulate decaying blast waves such as are encountered in nuclear explosions, by releasing compressed, heated gas from a number of bottle-shaped, high-pressure steel driver tubes, also called blast generators. Each blast generator is equipped with a double-diaphragm system in the bottle neck through which the gas exits into a large expansion tunnel. By judiciously choosing the initial driver conditions of volume, pressure, temperature and throat area, a blast wave of desired shock overpressure and weapon yield can be simulated. The concept of an LB/TS is illustrated in Figure 1b.

The planned U.S. LB/TS will have nine blast generators (1). They are anchored in the ground by a massive concrete reaction pier (2). Each of these blast generators will have an inside diameter of 1.83 m and a maximum length of 41 m. The upstream end of each tube is closed by a hydroplug which may be moved back and forth along the inside of the driver tube in order to adjust the driver volume. At the downstream end, the cylindrical driver tubes are equipped with a convergent nozzle (3) and a throat section of 0.914 m in diameter which houses the double-diaphragm system. The flow cross section in the throat can be reduced by installing a baffle plate in the upstream diaphragm location to further retard the outflow of the gas and obtain longer flow durations at low shock pressures. Nitrogen is used as driver gas. It is stored in liquid form (15) and, prior to a test, forced by cryogenic pumps (17) through four pebble-bed superheaters (16) (Osofski, Mason, and Tanaka 1991) into the driver tubes.

The 171-m-long expansion tunnel (5) is formed of pre-stressed concrete and has a semi-circular cross section of 162 m^2. This size is deemed necessary to avoid blocking of the flow about the largest target (Ethridge et al. 1984). The test section for the targets (11) is 18 m deep and centered at about 107 m downstream from the exit of the driver nozzles into the expansion tunnel. The thermal radiation effect associated with a nuclear explosion will be effected through the combustion of a mixture of aluminum powder and oxygen near the target (6). Four thermal radiation sources (TRS) will be mounted in the tunnel floor (7) forward of the test section, and the combustion products will be evacuated through exhaust fans, called ejectors (8), mounted in the tunnel roof (Guest 1989; Haasz and Gottlieb 1987).

An active RWE will be mounted at the open end of the expansion tunnel (14) to prevent the formation of reflecting shocks or rarefaction waves (Guice, Butz, and Gottlieb 1991). These reflections travelling upstream into the expansion tunnel would destroy the shape of the simulated blast wave once they reach the test section. The RWE is called active because its rotating vanes continuously adjust the available exit flow area in a controlled manner during the entire duration of the test. The motion of the vanes is controlled computationally, and the control function has to be known before the test. The control function, however, depends on the size and shape of the blast wave which is to be simulated and can only be generated once the experimental blast wave is known. Since this information becomes available only after the test, an accurate computational prediction of the expected experimental blast wave is needed from which the control function for the RWE is determined and empirically improved later on as experimental data become available.
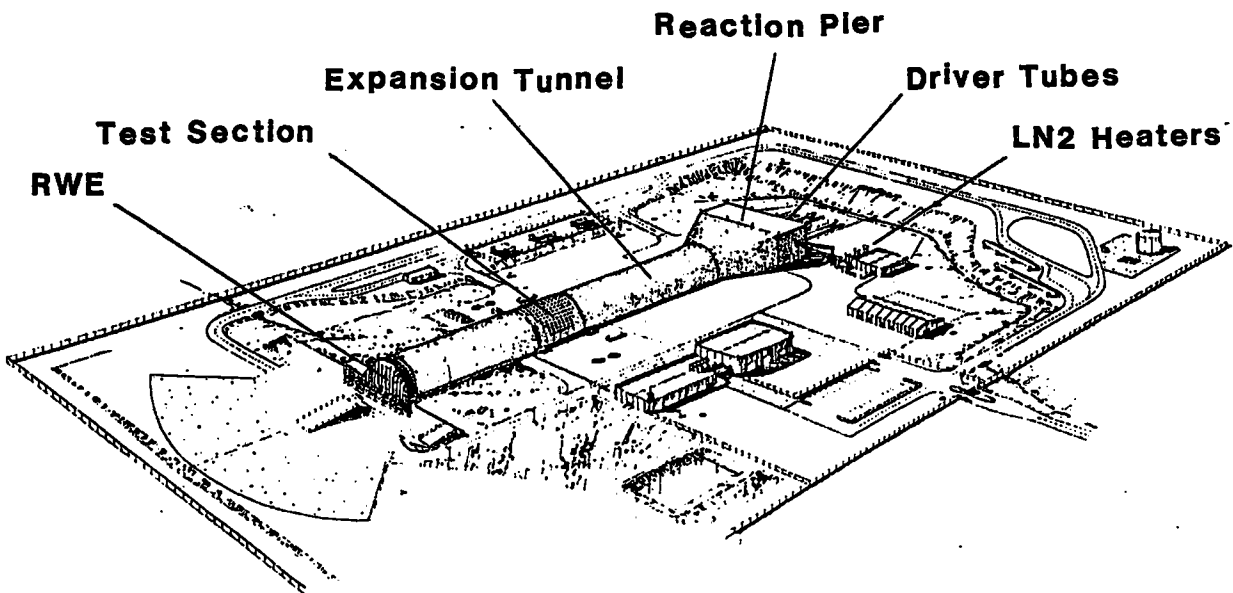
(a) Layout of the LB/TS Facility.
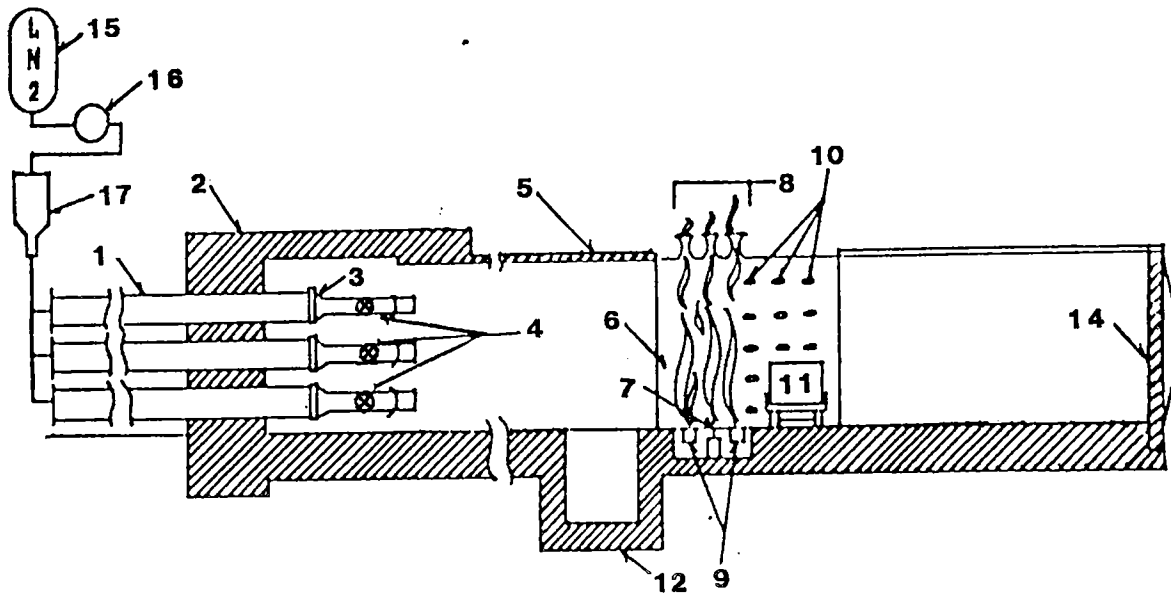
LEGEND

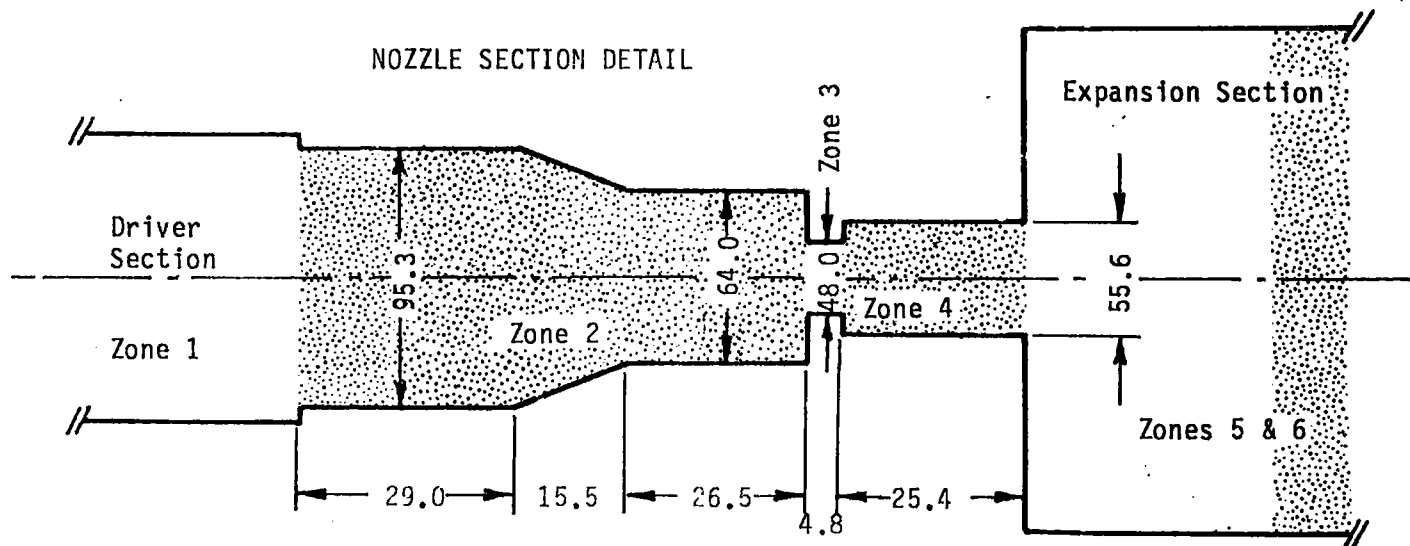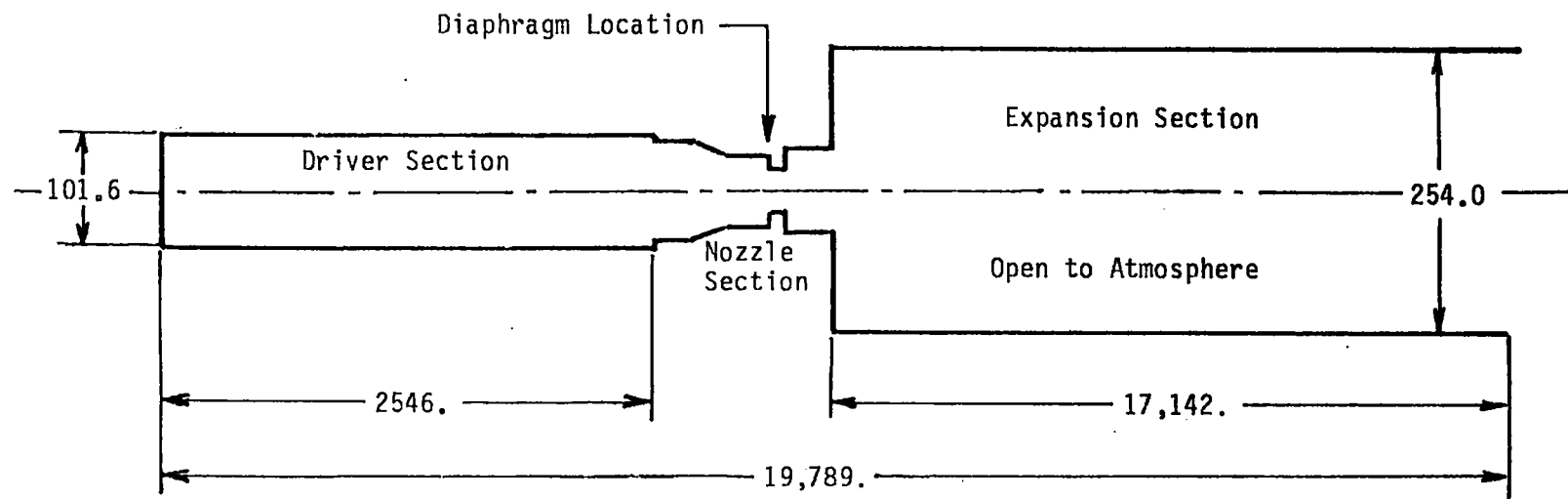|	
1 - Steel Driver Tubes	9 - Air Curtain Plenum
2 - Concrete Reaction Pier	10 - Instrumentation and Light Ports
3 - Converging Nozzles	11 - Test Target
4 - Diaphragms (or Throat Valves)	12 - Soil Tank (eliminated)
5 - Concrete Expansion Tunnel	14 - Rarefaction Wave Eliminator
6 - Steel Test Section	15 - Liquid Nitrogen Storage
7 - Thermal Radiation Sources	16 - Cryogenic Pumps
8 - Combustion Products Ejectors	17 - Pebble-Bed Superheaters

(b) The BRL LB/TS Concept

Figure 1: The U.S. Large Blast/Thermal Simulator (LB/TS) Design Concept.

3. Experimental Blast Simulator Studies

Initially, the U.S. design was based on the Large Blast Simulator (LBS) at the Centre d'Etudes de Gramat (CEG), France (Cadet and Monzac 1981). However, it soon became clear that a much larger facility was needed in order to accommodate the full range of anticipated targets without blocking the flow about the targets (Ethridge et al. 1984). Also, a broader range of shock overpressures and weapon yields was needed to cover the test conditions specified by the U.S Army. Since experimental model facilities of the planned LB/TS were not readily available, BRL relied on a fairly simple, quasi-one-dimensional computational model (BRL-Q1D) to develop the conceptual design of the LB/TS (Mark and Opalka 1986). The results of the computational studies with the BRL-Q1D code by this author (Opalka 1987/89) showed that the full-scale LB/TS facility must employ driver gas heating, an active RWE, and should use divergent nozzles and computer-controlled throat valves to optimize control and operation of the facility. However, for reasons of cost, the divergent nozzles were eliminated from the design, and the valve concept was abandoned by DNA in favor of the proven diaphragm technique.

Experimental efforts were initiated at the onset of the research project in 1982, but test results became available only much later because the construction of the model facility required a long time. To date, small-scale experiments with cold and heated driver gas, as well as an active RWE model, have been completed and the results have been used to validate computational predictions (Hisley et al. 1985; Coulter 1987; Gion 1989; Schraml and Pearson 1990). A throat-valve model has been built and initial tests were performed for the validation of the design concept and of the computational predictions (Stacey 1992). Also, a 1/6-scale LB/TS using a double diaphragm and an active RWE is under construction at ARL and will be used for validating the design concepts, for phenomenological research and for vulnerability testing of small items of military equipment once the characterization of the facility is completed.

A 1:57-Scale LBS model without thermal radiation capability has been used quite extensively at BRL to study flow phenomena in an LB/TS-type shock tunnel (Coulter 1987). The axisymmetric configuration was chosen for reasons of simplicity in construction and operation and in view of the availability of numerical data from one- and two-dimensional axisymmetric Computational Fluid Dynamics (CFD) codes. The simulator model consists of a number of interchangeable cylindrical driver tubes of 101.6 mm inner diameter and various lengths, a converging nozzle section, a throat section with diaphragm holder, and a very long (17,142 mm), open-ended expansion section. Strip heating elements are wrapped around the 2,546-mm-length driver so that the high-pressure driver gas can be heated. The purpose of Coulter's (1987) experiments was to demonstrate the effect of driver gas heating on the shape of decaying blast waves simulated in shock tunnels. His results have since been used to evaluate one- and two-dimensional axisymmetric CFD codes (Coulter 1987; Hisley 1990; Schraml 1991) and to validate computational performance predictions for the US-LB/TS. From Coulter's experiments, a test case was selected for evaluating and validating the USA-RG2 code results. The initial test conditions in the 1:57-Scale LBS model for the selected test case are listed in Table 1. The geometry of the 1:57-Scale LBS model used in the numerical formulation of the problem is defined in Figure 2.

Diaphragm Location

Expansion Section

Driver Section

—101.6—   —254.0—

Nozzle
Section

Open to Atmosphere

2546.

17,142.

19,789.

NOZZLE SECTION DETAIL

Zone 3

Expansion Section

Driver
Section

95.3   64.0

48.0   55.6

Zone 1

Zone 2

Zone 4

Zones 5 & 6

29.0   15.5   26.5   25.4

4.8

All Dimensions in millimetre - Not to Scale

Figure 2: Schematic of the 1:57-Scale Large Blast Simulator (LBS) Model.

5

Table 1. Initial Test Conditions			
driver pressure	= 15,032.5 kPa	driver temperature	= 570.15 K
ambient pressure	= 102.5 kPa	ambient temperature	= 296.15 K

The available experimental data are the stagnation pressure and the static pressure versus time. For measuring these data, two pressure probes were located at 442.5 cm from the beginning of the expansion tunnel in the downstream axial direction. At this location, the static pressure probe was mounted flush with the wall of the expansion tunnel, 12.7 cm in the radial direction from the axis of symmetry, and the stagnation pressure probe was mounted at the half radius, 6.35 cm from the axis of symmetry pointing in the upstream axial direction. This latter position is called Gage-8.

The data were recorded using an analog to digital conversion program installed in a Zenith model 248 microcomputer which permits sampling at a maximum rate of 60,000 samples per second per channel. Up to 16 data channels may be recorded simultaneously with this setup. The time and voltage samples are written to a 12-bit binary disc file and later converted to ASCII format. A data reduction program was then used to convert voltages into pressures.

From the two measurements of stagnation pressure, p_0, and the static pressure, p, the Mach number, M, and the dynamic pressure, q, can be computed (Liepmann and Roshkow 1957, pp 148-149). The Mach number has to be determined first because the dynamic pressure depends on it.

$$q \equiv \frac{1}{2}\rho u^2 = \frac{\gamma}{2}pM^2 \qquad (3\text{-}1)$$

For subsonic flow, the well-known isentropic relation between the static pressure and the Mach number may be used,

$$\frac{p_{01}}{p} = \left[1 + \frac{\gamma - 1}{2}M^2\right]^{\gamma/(\gamma - 1)} \qquad (3\text{-}2)$$

where the pitot pressure, p_{01}, equals the stagnation pressure.

For supersonic flow, Rayleigh's supersonic pitot formula must be used because the indicated pitot pressure, p_{02}, is the stagnation pressure behind the normal shock standing in front of the pitot probe.

$$\frac{p}{p_{02}} = \left[\frac{2\gamma}{\gamma + 1}M^2 - \frac{\gamma - 1}{\gamma + 1}\right]^{1/(\gamma - 1)} \cdot \left[\frac{\gamma + 1}{2}M^2\right]^{-\gamma/(\gamma - 1)} \qquad (3\text{-}3)$$

Since Equation (3-3) has no solution by quadratures, Newton's iterative method is used to determine the Mach number. The dynamic pressure is then obtained from the static pressure and the Mach number using Equation (3-1).

4. Blast-Wave Simulations With the USA-RG2 Code

The Unified Solution Algorithm (USA) codes were developed at the Rockwell International Science Center (RISC) under the leadership of Dr. Sukumar Chakravarthy (1986,1988). The USA codes are a series of hydrodynamic codes capable of solving numerically a large variety of fluid dynamic problems. Either the Euler equations or the Navier-Stokes equations in their Reynolds-averaged form may be solved in two (Cartesian and axisymmetric) or three dimensions. Implicit solution algorithms using the approximate factorization method or the Gauss-Seidel relaxation method are coded. The explicit, multistage Runge-Kutta method may be used to solve the governing equations in either space-marching or in time-dependent mode. The USA codes can treat calorically and thermally perfect gases, equilibrium-chemistry gases, and finite-rate reacting gases (Palaniswamy, Chakravarthy, and Ota 1989), and the user may define an arbitrary number of species and types of chemical reactions.

The governing equations are cast into finite-volume difference form for the conservation of flux, using an upwind Total Variation Diminishing (TVD) formulation for their convective terms (Chakravarthy et al. 1985). This discretization assures up to third-order accuracy in space and first-order accuracy in time. The TVD formulation guarantees solutions free of oscillations and keeps the numerical dissipation to a minimum. Roe's approximate Rieman solver is favored among several available Riemann solvers for defining fluxes at all cell faces. Turbulence may be modeled in various ways, including a zero-equation, modified Baldwin-Lomax model; a one-equation, $k-L$ model; and a two-equation, $k-\varepsilon$ model. All turbulence models are augmented by a separation model that has the capability to treat the recirculating flow in regions of flow separation. A multizone structured grid facilitates the treatment of complex, three-dimensional geometries (Szema, et al. 1988). Boundaries may be specified from point to point in the grid using either templates or user-supplied subroutines.

The computational grid for the 1:57-Scale LBS model is made up of five or six zones. The zones are indicated in Figure 2 which defines the geometry of the problem. The cylindrical driver tube forms the first zone. The nozzle region is subdivided into three zones: Zone 2 lies upstream of the diaphragm, Zone 3 is the baffle area next to the diaphragm, and Zone 4 lies downstream of the throat baffle. The expansion tunnel is divided into two zones, in order to conserve disc storage space and computing time. Zone 5, which contains the pressure probe locations 1 thru 9, is fully gridded in x- and y-direction. Zone 6 is a long region with few exponentially expanding grid points in the x-direction. The only purpose of Zone 6 is to move the transmissive end boundary far downstream from Zone 5 and the pressure probe locations.

An analytical grid generator, allowing clustering of the grid points near the boundaries in axial and radial directions, was supplied by RISC. The clustering function spaces the grid points in an exponentially expanding series with clustering either on one or on both ends of the zone. The first and last cell dimensions in each zone next to a boundary, ΔX_{min} and ΔY_{min}, are written into the subroutine as user-defined constants. The dimensions used in the present case are $\Delta X_{min,1} = 0.1$, $\Delta X_{min,2} = 0.01$, $\Delta Y_{min,1} = 0.1$ for the inviscid solution, and $\Delta Y_{min,1} = 0.001$ for the viscous solutions. $\Delta X_{min,2}$ is used with

7

Zone 3 on both ends, and $\Delta X_{min,1}$ is used with the remaining zones on both ends except the last zone. For the last zone, either Zone 5 or Zone 6, as the case may be, the grid points are clustered in axial direction using $\Delta X_{min,1}$ at the upstream boundary only.

Four grid variations are used in this study identified as the 5-zone coarse, 6-zone coarse, 5-zone fine, and 6-zone fine grids. The grid sizes for Zones 1 thru 6 are defined in Table 2 with the total number of grid points ranging from 8,400 for the 5-zone coarse grid to 15,550 for the 6-zone fine grid. The 5-zone coarse grid is considered the base-line grid against which the results from other grids are compared. It is modified further by lengthening Zone 5 of the modeled expansion tunnel from 5.00 to 10.00 and 15.00 m and increasing the number of grid points in axial direction from 60 to 120. The fine grids are employed to compare the computational results to those obtained with the coarse grids and to study their effect on the flow solution. The refinement consists in increasing the number of grid points in radial direction by a multiplicative factor of 1.25 so that more grid points are placed near the walls inside the boundary-layer regions. The length of Zone 5 is 9.00 m in the 5-zone grid and 5.00 m in the 6-zone grid with 120 or 100 grid points in the axial direction. The 6-zone grids are employed versus the 5-zone grids to evaluate the influence of the transmissive end boundary on the numerical results.

Table 2. Grid Sizes				
Zone	Coarse Grids		Fine Grids	
5	5.00 m	10./15. m	5.00 m	9.00 m
1	50x50	50x50	50x60	50x60
2	30x40	30x40	30x50	30x50
3	10x20	10x20	10x25	10x25
4	30x30	30x30	30x40	30x40
5	60x60	120x60	100x80	120x80
6	20x60	0	20x80	0
Total	9,600	12,000	15,550	15,550

The objective of the present investigation is to evaluate the quality of the computational prediction by comparing the numerical results to the available experimental data. The approach taken is to proceed from the inviscid USA-RG2 solution to the more complex viscous solutions. The inviscid Euler equations are solved first, then the viscous Navier-Stokes equations for laminar flow are solved. After that, the turbulence models are evaluated, ending with the most complex viscous solution invoking the k-ε turbulence model. In order to conserve computing time, the CFL number (Courant-Friedrichs-Lewy stability criterion) was ramped up from unity as quickly as possible until a maximum was found at which each solution would execute. Table 3 shows the various CFL ramps for the perusal of those readers who wish to reproduce the results of the present studies. The studies described below were performed using the test case selected from the 1:57-Scale LBS model experiments (Table 1).

Table 3. CFL Ramps for 5-Zone and 6-Zone Grids									
Coarse Grids								Fine Grids	
Inviscid		Visc-Laminar		V-Turbulent(1)		V-Turbulent(2)		All Viscous	
NT>	CFL	NT>	CFL	NT>	CFL	NT>	CFL	NT>	CFL
0	0.1	0	1	0	0.01	0	1	0	1
10	1.0			10	0.1				
20	5.0	20	10	30	1.0			20	10
50	10.			50	10.	100	10	100	20
100	25.	90	25	90	25.	200	20	200	40
150	50.	180	50	180	50.	300	30	300	60
		270	75	270	75.				
		360	100	360	100				
		450	150	450	150	1800	180	800	160
		540	200	550	200	1900	190	900	180
						2000	200	1000	200
		12000	150	9000	150			1500	250*
								*6-zone grid only!	

4.1 Influence of Grid Coarseness on Numerical Solution

Three inviscid computations with varying grid coarseness in Zone 5 were executed. The grid in Zone 5 of the expansion tunnel, in which the pressure probes are located, is varied in axial direction from 5.00 m and 60 grid points to 10.00 m and 120 grid points, and from there to 15.00 m and 120 grid points keeping ΔX_{min} unchanged. Because the grid points are clustered exponentially toward the boundaries in axial direction, the second grid is coarser in the interior of the zone than the base-line grid. Figure 3 shows the results of these computations compared to the available experimental data. The stagnation pressure, static overpressure, and dynamic pressure are plotted versus time. Such flow representations are called pressure histories.

Two typical phenomena of inviscid shock tube flow solutions found in the pressure histories in Figure 3 are the sudden pressure drop behind the shock and the general underprediction of the static overpressure. These phenomena have also been observed in the numerical results gained from other CFD codes (Opalka and Mark 1986; Hisley 1985,1988,1990; Schraml 1991). It is further learned, that the coarser grids generated by lengthening Zone 5 cause major deviations of the pressure histories from those for the base-line grid (zone 5 = 5.00 m). The increased grid coarseness in Zone 5 causes an unrealistic resurgence of the dynamic pressure between 12 and 22 ms, with the dynamic pressure rising to values 120 percent of the pressure at the shock front. The comparison shows that the coarser the grid, the the stronger the resurgence of the dynamic pressure will be. This resurgence of the dynamic pressure, like the sudden pressure drop mentioned above, does not appear in the following viscous solutions and has to be attributed to the

USA-RG2 Inviscid Solution for 1:57-Scale LBS Model"
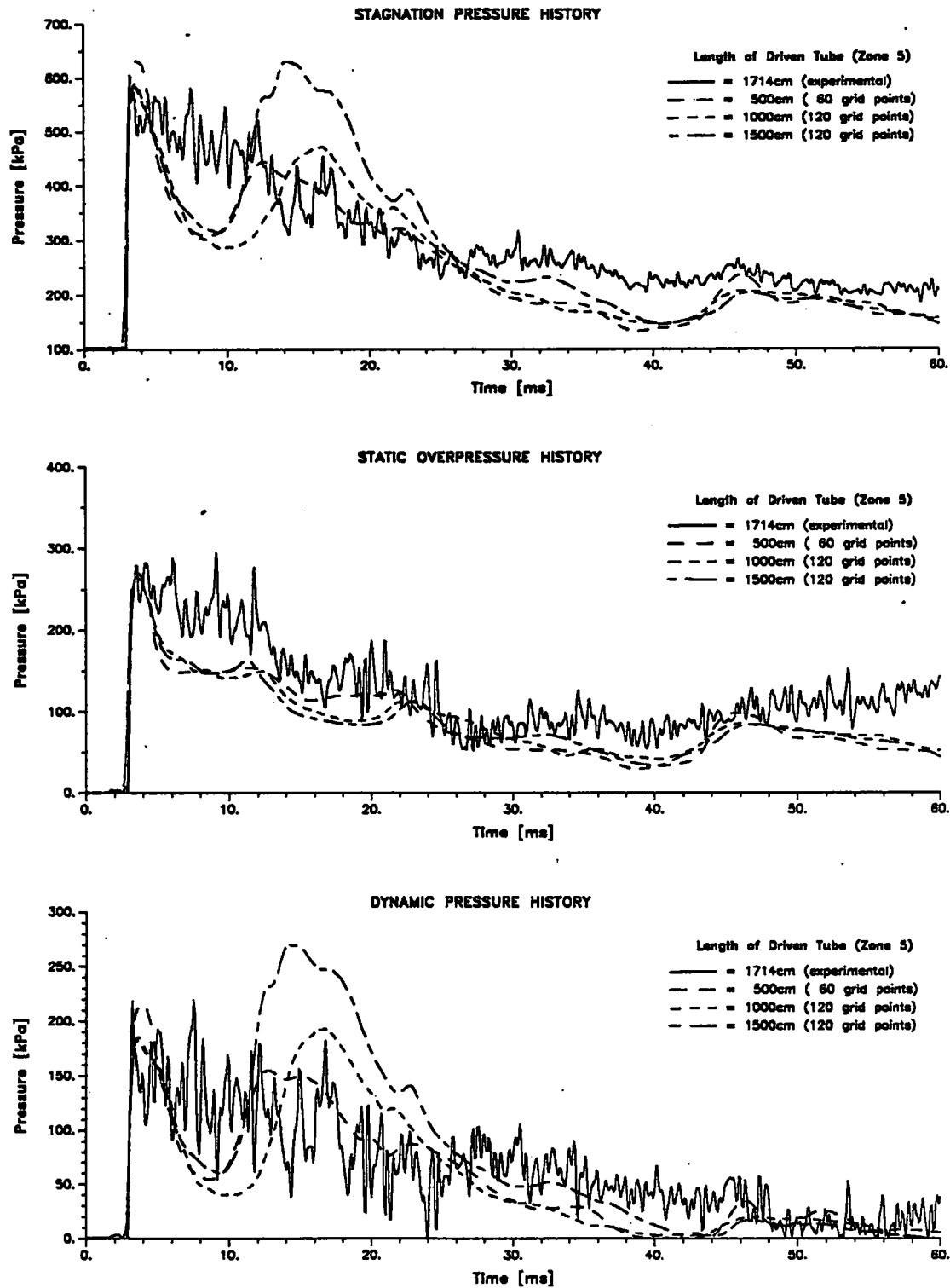## Gage-8 (x,y = 442.5,6.35 cm)

Figure 3. Effect of Grid Coarseness on Numerical Solution.

inviscid modeling of the flow solution. The conclusion is in this case that the base-line grid is the coarsest possible to obtain a reasonable inviscid solution.

The question presented itself whether or not a refined grid would improve the solution obtained with the base-line grid. This question was investigated choosing the laminar-viscous solution provided in the USA-RG2 code by solving the Navier-Stokes equations without turbulence. Figure 4 shows the results of these computations comparing the pressure histories computed with the base-line 5-zone coarse grid to the pressure histories obtained with the 5-zone and 6-zone fine grids. The most significant difference to the inviscid solution is the absence of the depression region behind the shock front. The static overpressure is less underpredicted by the laminar-viscous solution than by the inviscid solution. The refined grid offers the best simulation of the pressure histories, although a slight overprediction of the dynamic pressure, especially between 18 ms and 27 ms, exists. Overall, the laminar-viscous pressure predictions obtained with the 6-zone fine grid appear to follow the experimental data most closely.

4.2 Comparison of Three Turbulence Models

The USA-RG2 code contains three turbulence models known as zero-equation, one-equation, and two-equation models referring to the number of partial differential equations (PDEs) they employ. They differ in the method of determining the eddy viscosity which is the turbulent contribution to the viscosity coefficient used in the viscous diffusion terms of the Navier-Stokes equations. The eddy viscosity, v, is calculated in all three models from

$$v_t = V \cdot L \qquad (4\text{-}1)$$

where V is the velocity scale function and L is a length scale function. To model the turbulence in detached flow regions, an algebraic backflow model (Ramakrishnan and Goldberg 1990) is built-in as a module with each of the three turbulence models.

The zero-equation model (Goldberg 1986) is an algebraic, modified Baldwin-Lomax (MBL) formulation which uses two algebraic scaling functions for the mean velocity and location to determine the eddy viscosity distribution. A two-layer approach is used to treat turbulence-producing shear flow surfaces. The inner layer formulation is used near the shear flow surface and a damping function accounts for the attenuation of turbulence in the near-wall regions when the surface is solid. Farther away from the surface, the outer layer formulation is employed.

The one-equation model (Goldberg and Chakravarthy 1990) uses the solution of one PDE for the kinetic energy of turbulence, k, to determine the velocity scale such that

$$V = \sqrt{k} \qquad (4\text{-}2)$$

and retains the algebraic form of a rather complicated length scaling function to determine the eddy viscosity distribution. It is also called the k-L model.

11

USA-RG2 Laminar-Viscous Solution for 1:57-Scale LBS Model
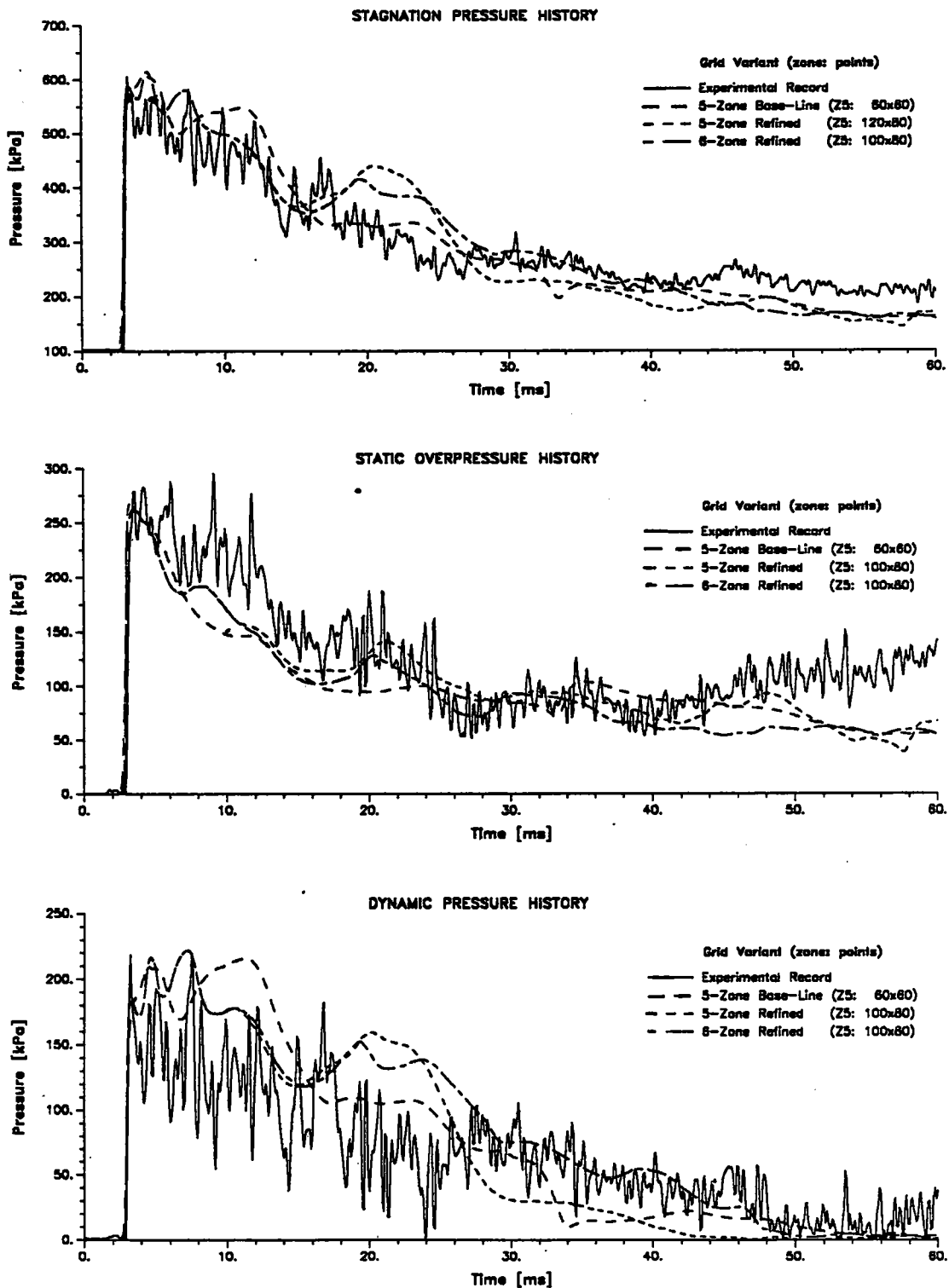### Gage-8 (x;y = 442.5;6.35 cm)

Figure 4. Effect of Refined Grid on Numerical Solution.

The two-equation model (Goldberg and Ota 1991) uses the solutions to two PDEs to determine the velocity and length scales for the determination of the eddy viscosity distribution. The first PDE for k is the same as in the one-equation model (Equation 4-2). The second PDE is for the isotropic part of the turbulence dissipation, ε, such that the length scale is

$$L = \frac{k^{1.5}}{\varepsilon}. \tag{4-3}$$

In this case, the eddy viscosity (Equation 4-1) becomes

$$v_t = \frac{k^2 \times D}{\varepsilon}, \tag{4-4}$$

where the damping function D includes solid wall effects. The two-equation model is also called the k-ε model.

The turbulence models are invoked through user-defined constants located in the input. The desired model is chosen according to the number of PDE's it uses, i.e., 0, 1, or 2. Additional constants permit the turning on or off of the viscous terms and the turbulent diffusion terms in the governing flow equations. The user can further set zonal input constants to identify turbulence-producing mechanisms like walls, wakes, etc.; invoke the separation model; define the transition point from laminar to turbulent flow; and select the separation viscosity, μ_{sep}. For the turbulent cases, the turbulence-generator flags are turned on along all wall boundaries, except when invoking the k-ε turbulence model. It seems that because there is a lot of initial boundary layer development in Zone 3, but inadequate grid resolution, the solution becomes unstable at moderate CFL numbers. In order to maintain stability of the solution with the k-ε turbulence model at higher CFL (≥ 200) numbers, the turbulence-generator flags in the axial direction are turned off in all zones except Zone 5, and the turbulence-generator flag in the radial direction is turned off in Zone 3. Also, the k- and ε-equation subroutines are modified to make the equations first-order accurate.

The stagnation, static, and dynamic pressure histories resulting from the application of the three turbulence models to the viscous flow solution are shown in Figure 5. The base-line 5-zone coarse grid was used in these computations. All three models produce good predictions of the shown pressure histories for the selected test case. The stagnation pressure history appears best simulated with the k-L model, while the static overpressure history seems simulated best with the MBL model. For the stagnation pressure history, the solution with the MBL model underpredicts and the solution with the k-ε model overpredicts the experimental record. For the static overpressure, the solution with the k-L model slightly underpredicts and the solution with the k-ε model slightly overpredicts the experimental record. The dynamic pressure is best simulated with the k-ε model solution. The solution with the k-L model overpredicts and the solution with the MBL model underpredicts the dynamic pressure. Since the dynamic pressure is the most sensitive parameter for evaluating the response of military equipment to drag forces which may cause overturning, it is concluded that the k-ε model is suited best for the computational prediction of the flow field in the 1:57-Scale LBS model.

USA-RG2 Turbulent-Viscous Solution for 1:57-Scale LBS Model
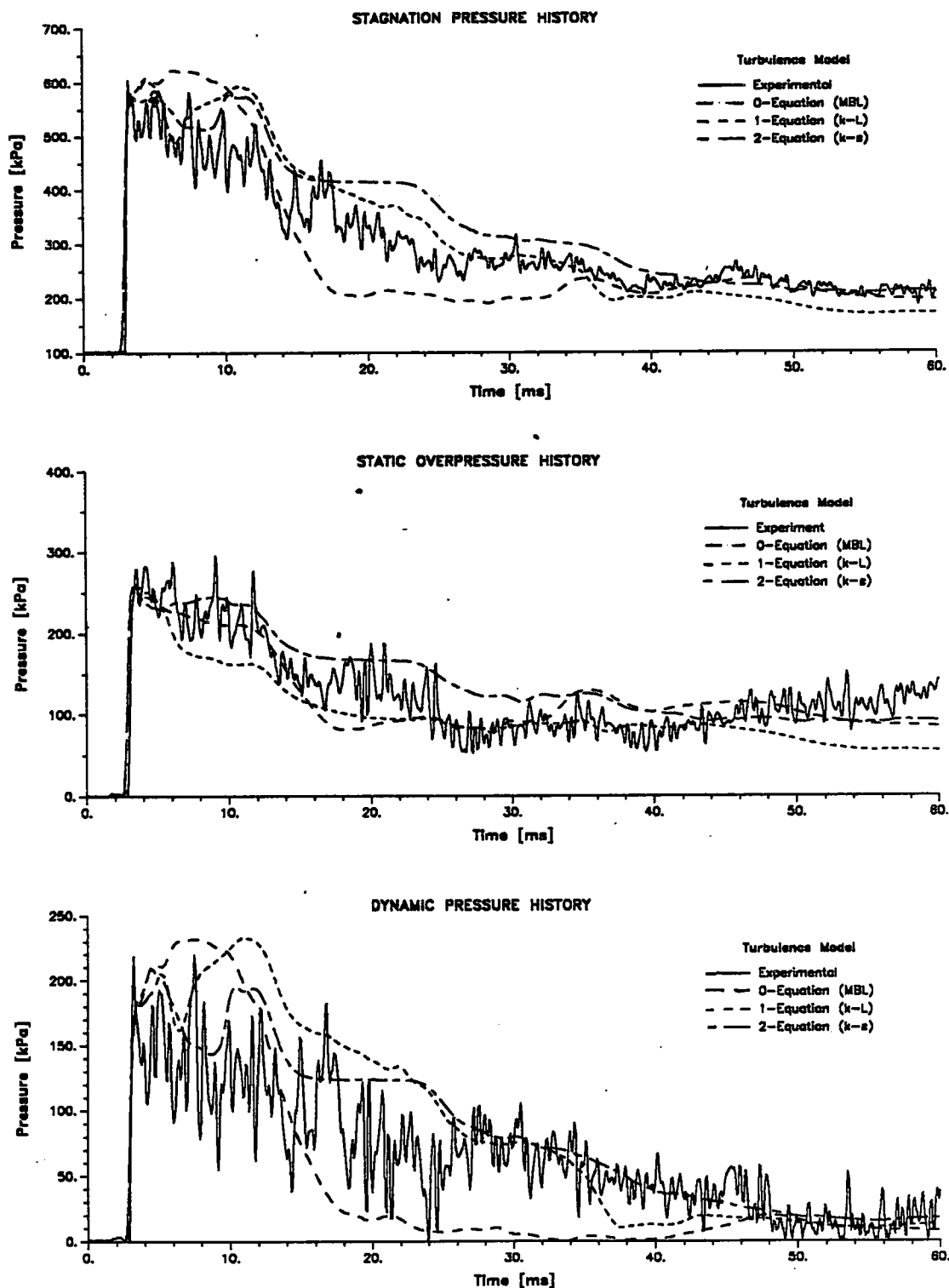Gage-8 (x,y = 442.5,6.35 cm)

Figure 5. Comparison of Three Turbulence Models in the USA-RG2 Code.

4.3 Influence of Transmissive Boundary on Solution

A question about the sufficiency of the base-line 5-zone coarse grid arises because the fifth grid zone, which represents the expansion tunnel of the 1:57-Scale LBS model, was limited to 5.00 m length by our consultants at RISC, whereas the actual length of the expansion tunnel is 17.14 m. The reasoning behind this shared decision is that the computation of the flow history in the expansion tunnel downstream from the pressure probe locations is not of interest to the observer. By not modeling this region of the expansion tunnel computing time and disk space can be saved. This approach is made possible by using a transmissive boundary at the end of the fifth zone which prevents any wave reflections back into the grid. To investigate the correctness of this procedure, a sixth zone is added to the base-line 5-zone grid which contains an equal number of grid points in radial direction as the fifth zone, but has only 20 grid points in axial direction (see Table 2), and the Euler inviscid solution algorithm is exercised for this inquiry.

When the pressure histories of the 5-zone versus the 6-zone coarse grids are compared, differences in the computational results become apparent. Figure 6 shows the comparison of the static overpressure histories for the two grids at two pressure probe locations 101.6 cm apart. At Gage-8, which is located nearest (57.5 cm) to the end boundary of the fifth grid zone, the two pressure histories differ one from another beginning after 8 ms of flow simulation (upper graph in Figure 6). At Gage 2, furthest (159.1 cm) from the end boundary of the fifth zone, the differences in the static overpressure histories begin only after 15 ms (lower graph in Figure 6). It is, therefore, concluded that the transmissive end boundary is not totally transparent but causes small reflections influencing the quality of the computational flow simulation.

To investigate the influence of the end boundary further, two special grids were constructed and applied to the viscous solution with the k-ε turbulence model invoked for the 1:57-Scale LBS model test case. The number of grid points was increased by a factor of 1.25 in the radial direction in all zones. Both grids have identical first through fourth zones (see Table 2). The fifth and the sixth zones have 80 grid points in the radial direction. In the axial direction, the fifth zone of the 5-zone extended grid has 120 grid points distributed over a 9.00 m length, and the fifth zone of the 6-zone refined grid has 100 grid points distributed over a 5.00 m length. Zone 6 has 20 grid points expanding in an exponential series distributed over a 12.14 m length. By comparing the solutions for the 5-zone base-line grid, the 5-zone extended grid, and the 6-zone refined grid it is hoped to demonstrate that the solution can be improved and that the disturbance from the end boundary can be eliminated.

The turbulent viscous solution was executed with each of the three grids, and the resultant histories of the stagnation, static and dynamic pressures are presented in Figure 7. All three grids yield satisfactory results. Within the same solution, in this case the viscous solution with k-ε turbulence model, the differences are really small. The noticeable differences exist between the pressure histories for the 5-zone base-line grid and the special, refined grids. The 5-zone extended grid and the 6-zone refined grid yield almost identical pressure histories. These results confirm that with the transmissive end boundary moved far downstream, similar grids yield nearly identical results. The 5-zone extended

grid improves the solution somewhat, and so does the 6-zone refined grid; but it remains doubtful whether or not the improved grid resolution warrants the additional effort in run time and cost for the larger, special grids.
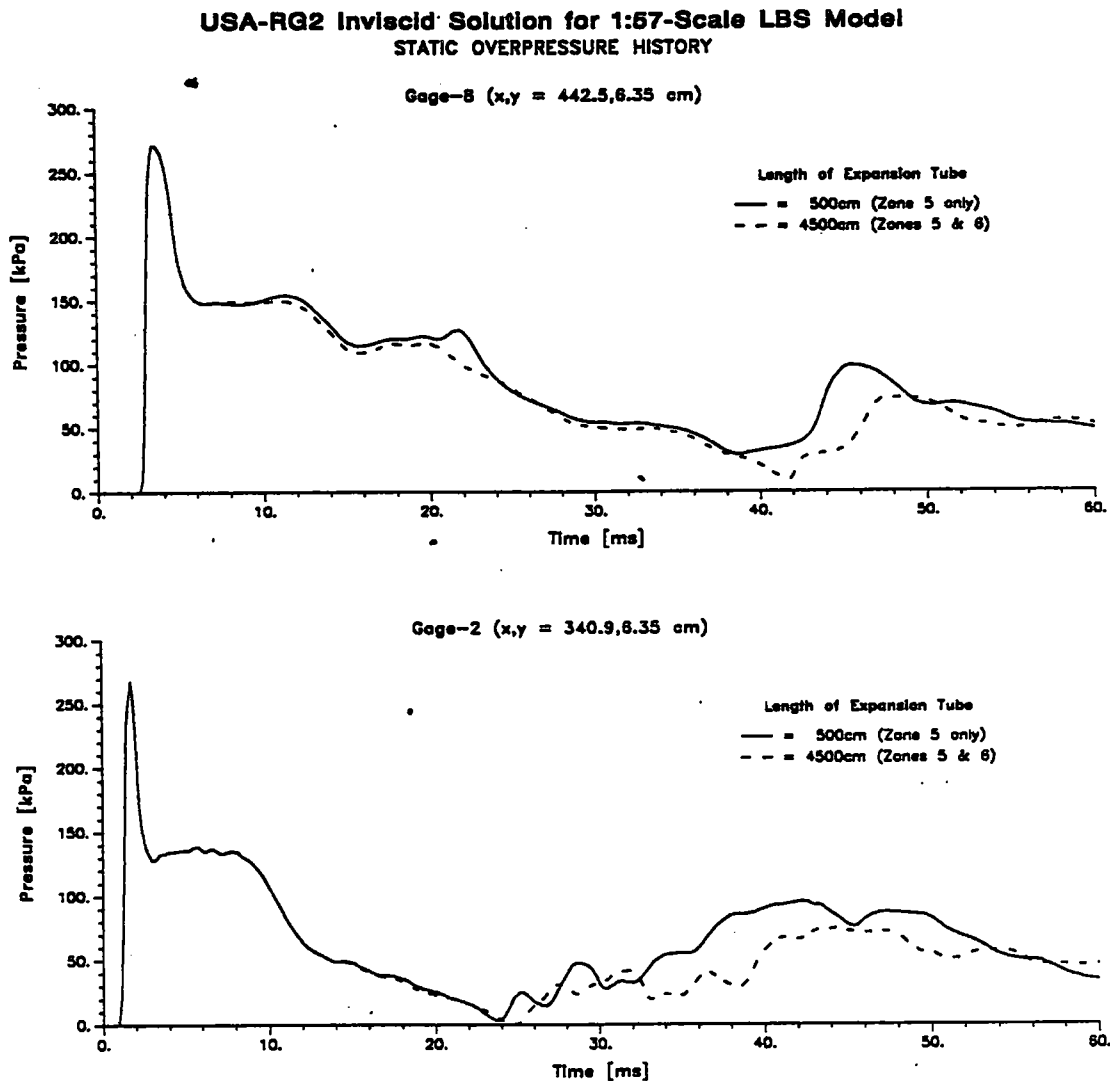

USA-RG2 Inviscid Solution for 1:57-Scale LBS Model
STATIC OVERPRESSURE HISTORY

Gage-8 (x,y = 442.5,6.35 cm)

Length of Expansion Tube
——— = 500cm (Zone 5 only)
– – – = 4500cm (Zones 5 & 6)

Gage-2 (x,y = 340.9,6.35 cm)

Length of Expansion Tube
——— = 500cm (Zone 5 only)
– – – = 4500cm (Zones 5 & 6)

Figure 6. Pressure Histories Obtained with 5-Zone and 6-Zone Coarse Grids.

4.4 Comparison of the Inviscid Versus the Viscous Solutions.

The more significant differences in the flow solutions exist between the inviscid, the laminar viscous, and the turbulent viscous solutions and between the three turbulence models (Figure 5). The stagnation, static and dynamic pressure histories for the inviscid, laminar viscous, and turbulent viscous solutions are compared in Figure 8. In all cases, a 6-zone grid was used in the computation. The Euler-Inviscid solution predicts the shock pressure at the front of the blast wave well but underpredicts the stagnation, static, and dynamic pressure histories and thereby the associated impulses which are represented by the area under the pressure history curve. Therefore, the inviscid solution predicts the pressure histories least accurately.

16

USA-RG2 Turbulent-Viscous Solution for 1:57-Scale LBS Model
Gage-8 (x,y = 442.5,6.35 cm)
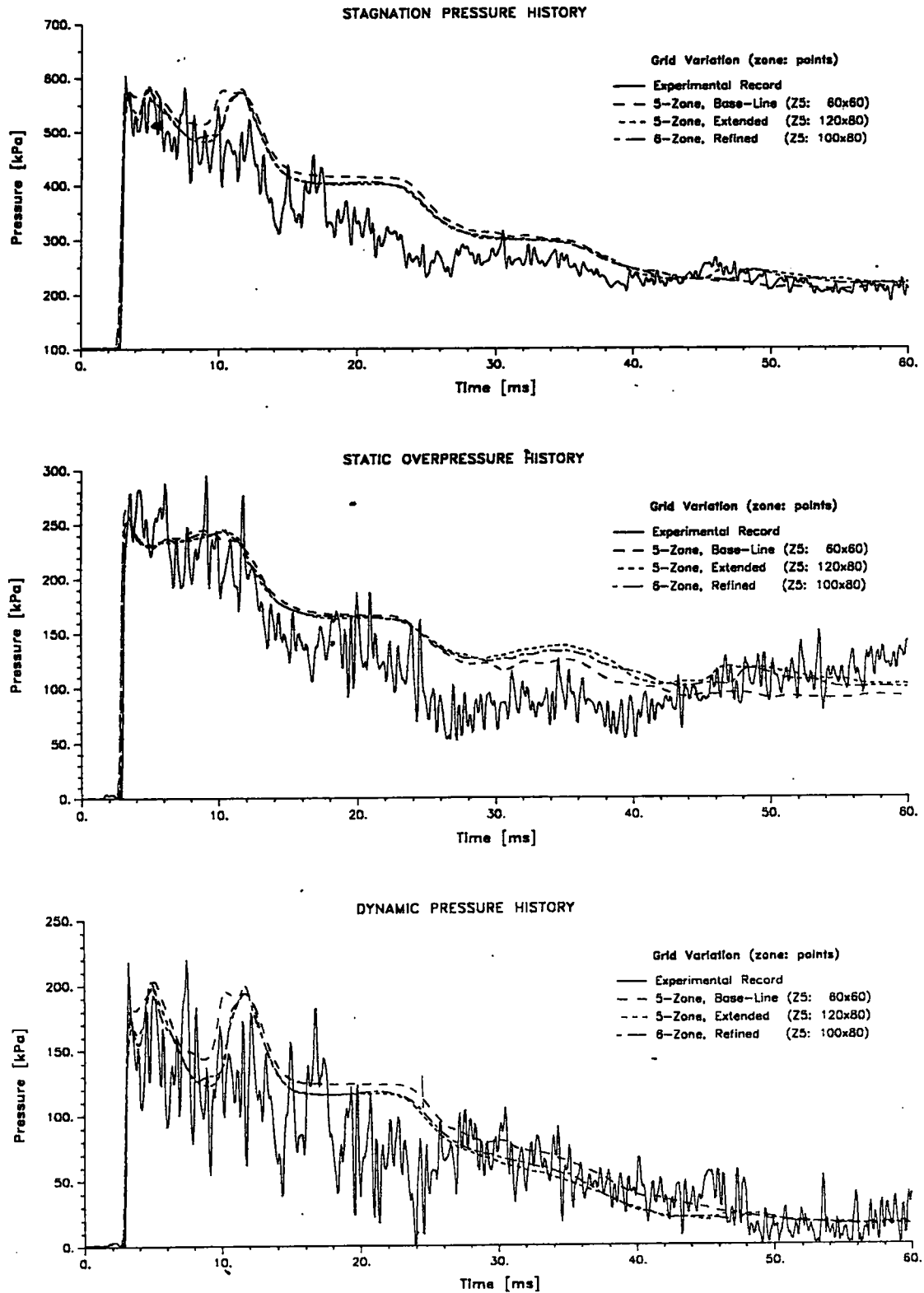
Figure 7. Effect of Grid Variations on the Numerical Solution
Using the k-ε Turbulence Model.

The laminar viscous solution yields a much improved prediction when compared to the inviscid solution, but underpredicts the static overpressure and the static-overpressure impulse, and overpredicts the dynamic pressure and the dynamic-pressure impulse. The turbulent viscous solution predicts the three pressure histories better than the inviscid or laminar viscous solutions. The best prediction is achieved with the k-ε turbulence model although this solution slightly overpredicts the experimental records.

5. Conclusions

The USA-RG2 code was evaluated for its capability of predicting and simulating decaying blast waves generated in a shock tunnel. Coulter's 1:57-Scale LBS Model and experimental records served as benchmark results for the evaluation. The comparison of the experimental and computational results proves that the USA-RG2 code can successfully simulate the available experimental pressure histories for stagnation, static, and dynamic pressure.

The USA codes are capable of modeling complex geometries by subdividing the geometry using a node-aligned multi-grid approach. It was found that the cell size in the grid can have a significant influence on the accuracy of the flow solution. By increasing the number of grid points by a factor of 1.25 in the radial direction, the solution could be improved.

It was learned that the transmissive end boundary is not totally transmissive, but influences the flow solution with time. To keep reflections from the end boundary to a minimum, it is preferable to model the expansion section of the 1:57-Scale LBS model with a 6-zone grid in its entire length rather than with a 5-zone grid for a short section, as was originally done in this project.

The best simulation was obtained for the viscous solution with the two-equation, k-ε turbulence model invoked, although this turbulence model slightly overpredicts the experimental record. If it is desirable to bracket the prediction, the laminar-viscous solution which underpredicts the experimental record may be executed.

USA-RG2 6-Zone Grid Solutions for 1:57-Scale LBS Model
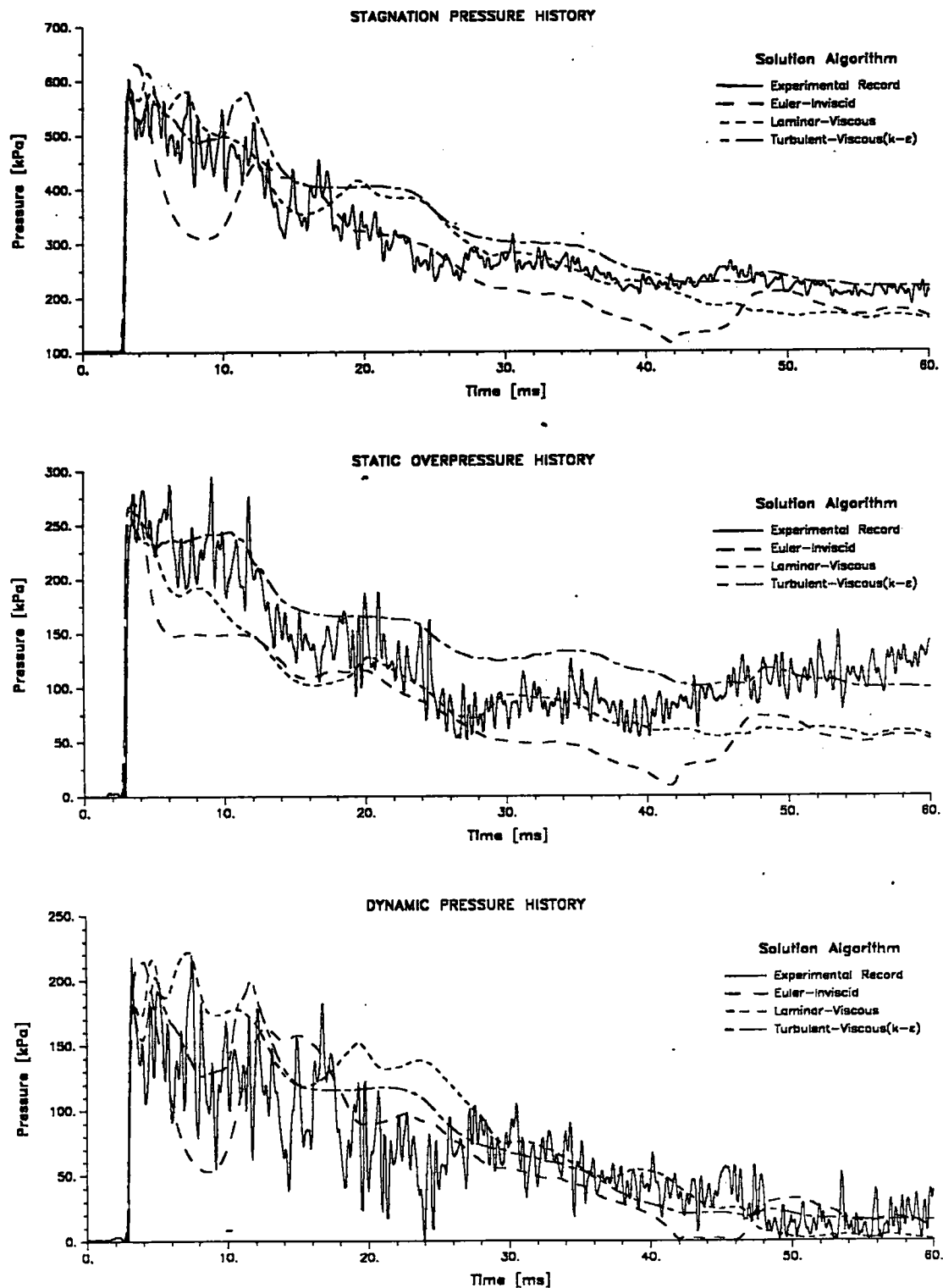## Gage-8 (x;y = 442.5;6.35 cm)

Figure 8. Comparison of the Inviscid, Laminar Viscous and Turbulent Viscous Numerical Solutions with Experimental Data.

References

Cadet, A., and J. B. G. Monzac. "The Large-Scale Nuclear-Blast Simulator of the Gramat Research Center: Description and Operational Utilization." <u>Proceedings of the Seventh International Symposium on the Military Application of Blast Simulation (MABS-7),</u> Vol. 1, Paper No. 1.2, Medicine Hat, Alberta, Canada, 13-17 July 1981.

Chakravarthy, S. R. "The Versatility and Reliability od Euler Solvers Based on High-Accuracy TVD Formulations." AIAA Paper No. 86-0243, 1986.

Chakravarthy, S. R. "High-Resolution Upwind Formulations for the Navier-Stokes Equations." Lecture Series 1988-05, Computational Fluid Dynamics, Von Karman Institute for Fluid Dynamics, March 1988.

Chakravarthy, S. R., K. Y. Szema, U. C. Goldberg and J. J. Gorski. "Application of a New Class of High Accuracy TVD Schemes to the Navier-Stokes Equations." AIAA Paper No. 85-0165, 1985.

Coulter, G. A. "Blast Parametric Study Using a 1:57 Scale Single Driver Model of a Large Blast Simulator." BRL-MR-3597, U.S. Army Ballistic Research Laboratory, Aberdeen Proving Ground, MD, June 1987.

Coulter, G.A., and R. J. Pearson. "Blast Parametric Study Using a 1:57 Scale Single Driver Model of a Large Blast Simulator - Part II." BRL-TR (to be published), U.S. Army Ballistic Research Laboratory, Aberdeen Proving Ground, MD.

Ethridge, N. H., R. E. Lottero, J. D. Wortman, and B. P. Bertrand. "Computational and Experimental Studies of Blockage Effects in a Blast Simulator." ARBRL-TR-02564, U.S. Army Armament Research and Development Center, Ballistic Research Laboratory, Aberdeen Proving Ground, MD, June 1984.

Gion, E. J. "A Multidriver Shock Tube Model of a Large Blast Simulator." BRL-MR-3757, U.S. Army Ballistic Research Laboratory, Aberdeen Proving Ground, MD, May 1989.

Goldberg, U. C. "Separated Flow Treatment with a New Turbulence Model." <u>AIAA Journal,</u> Vol. 24, No. 10, pp. 1711-1713, October 1986.

Goldberg, U. C., and S. R. Chakravarthy. "Separated-Flow Predictions Using a Hybrid k-L/ Backflow Model." <u>AIAA Journal,</u> Vol. 28, No. 6, pp.1005-1009, June 1990.

Goldberg, U. C., and D. K. Ota. "A k-ε Near-Wall Formulation for Separated Flows." AIAA Paper No. 90-1482, June 1990.

Gratias, S., and J. B. G. Monzac. "The Large-Scale Nuclear-Blast Simulator of the Gramat Research Center: Concept, Research, Performance." <u>Proceedings of the Seventh International Symposium on the Military Application of Blast Simulation (MABS-7),</u> Vol. 1, Paper No. 1.1, Medicine Hat, Alberta, Canada, 13-17 July 1981.

Guest, J. "Experiments in the Use of Ejectors to Remove Thermal Radiation Simulator Products from Blast Simulators." Proceedings of the 11th International Symposium on Military Applications of Blast Simulation (MABS-11), Albuquerque, NM, 10-15 September 1989.

Guice, R. L., J. Butz and J. J. Gottlieb. "Rarefaction Wave Eliminator Design Study." BRL-CR-678, U.S. Army Ballistic Research Laboratory, Aberdeen Proving Ground, MD, December 1991.

Haasz, A. A., and J. J. Gottlieb. "Venting od a Blast-Wave Simulator with a Linear Dual-Jet Air Curtain Phase II." Aerospace Engineering and Research Consultants Limited, Downsview, Ontario, Canada, DNA-TR-87-165, Defense Nuclear Agency, Washington, DC, 30 June 1987.

Hisley, D. M. "Computational Studies for 1/57-Scale Large Blast Simulator (LBS) Configurations With the BLAST2D Code." BRL-TR-3152, U.S. Army Ballistic Research Laboratory, Aberdeen Proving Ground, MD, September 1990.

Hisley, D. M., E. J. Gion, and B. P. Bertrand. "Performance and Predictions for a Large Blast Simulator Model." BRL-TR-2647, U.S. Army Ballistic Research Laboratory, Aberdeen Proving Ground, MD, April 1985.

Hisley, D. M., and G. A. Molvik. "Axisymmetric Calculations for the Large Blast/Thermal Simulator (LB/TS) Shock Tube Configuration." BRL-TR-2935, U.S. Army Ballistic Research Laboratory, Aberdeen Proving Ground, MD, September 1988.

Liepmann, H. W., and A. Roshko. Elements of Gasdynamics. John Wiley & Sons, Inc., New York, NY and London, GB, 1957, Fifth Printing, October 1963.

Mark, A., K. O. Opalka, C. W. Kitchens, G. A. Coulter, G. Bulmash and C. N. Kingery. "Simulation of Nuclear Blasts with Large-Scale Shock Tubes." Proceedings of the Eighth International Symposium on Military Applications of Blast Simulation (MABS-8), Spiez, Switzerland, 20-24 June 1983.

Opalka, K. O. "Large Blast-Wave Simulators (LBS) With Cold-Gas Drivers: Computational Design Studies." BRL-TR-2786, U.S. Army Ballistic Research Laboratory, Aberdeen Proving Ground, MD, March 1987.

Opalka, K. O. "Large Blast and Thermal Simulator Advanced Concept Driver Design by Computational Fluid Dynamics." BRL-TR-3026, U.S. Army Ballistic Research Laboratory, Aberdeen Proving Ground, MD, August 1989.

Opalka, K. O., and A. Mark. "The BRL-Q1D Code: A Tool for the Numerical Simulation of Flows in Shock Tubes with Variable Cross-Sectional Areas." BRL-TR-2763, U.S. Army Ballistic Research Laboratory, Aberdeen Proving Ground, MD, October 1986.

Opalka, K. O., and R. J. Pearson. "Real Time Flow Control in Large Blast/Thermal Simulators." Proceedings of the 1988 Army Science Conference, Ft. Monroe, Hampton, VA, 25-28 October 1988.

Opalka, K. O., and R. J. Pearson. "CFD Design Studies of an Advanced Concept Driver for a Large Blast/Thermal Simulator." Yong W. Kim (Ed.), AIP Conference Proceedings 208, Current Topics in Shock Waves. pp. 885-890, 17th International Symposium on Shock Waves and Shock Tubes, Lehigh University, Bethlehem, PA, 17-22 July 1989.

Opalka, K. O., and R. J. Pearson. "Advanced Design Concepts for a Large Blast/Thermal Simulator." Proceedings of the Eleventh International Symposium on Military Applications of Blast Simulation (MABS-11). pp. 85-95, Marriott Hotel, Albuquerque, NM, 10-15 September 1989.

Osofsky, I. B., G. P. Mason, and M. J. Tanaka. "Development of a Pebble-Bed Liquid-Nitrogen Evaporator and Superheater for the Scaled Large Blast/Thermal Simulator Facility." BRL-CR-661, U.S. Army Ballistic Research Laboratory, Aberdeen Proving Ground, MD, April 1991.

Ota, D. K., and U. C. Goldberg. "Computation of Supersonic Turbulent Shear Layer Mixing with Mild Compressibility Effects." AIAA Journal, Vol. 29, NO. 7, pp. 1156-1160, July 1991.

Palaniswamy, S., S. R. Chakravarthy and D. K. Ota. "Finite Rate Chemistry for USA-Series Codes: Formulation and Applications." AIAA Paper No. 89-0200, 1989.

Pearson, R. J. "Large Blast/Thermal Simulation." SAE Technical Paper #871746, Society of Automotive Engineers, 400 Commonwealth Drive, Warrendale, Pennsylvania, October 1987.

Pearson, R. J., K. O. Opalka, and D. M. Hisley. "Design Studies of Drivers for the US Large Blast/Thermal Simulator." Proceedings of the Ninth International Symposium on Military Applications of Blast Simulation (MABS-9). Vol. 1, Paper No. I.6, Southend-on-Sea, Essex, England SS3 9XE, September 1985.

Ramakrishnan, S. V., and U. C. Goldberg. "Versatility of an Algebraic Backflow Turbulence Model." AIAA Paper 90-1485, 1990.

Schraml, S. J. "Performance Predictions for the Large Blast/Thermal Simulator Based on Experimental and Computational Results." BRL-TR-3232, U.S. Army Ballistic Research Laboratory, Aberdeen Proving Ground, MD, May 1991.

Schraml, S. J., and R. J. Pearson. "Small Scale Shock Tube Experiments Using a Computer Controlled Active Rarefaction Wave Eliminator." BRL-TR-3149, U.S. Army Ballistic Research Laboratory, Aberdeen Proving Ground, MD, September 1990.

Schraml, S. J., and R. J. Pearson. "Distribution of Flow Across the Radius of an Axisymmetric Shock Tube with Variable Cross Sectional Area." Conference Proceedings of the CIE '91,

Stacey, M. R. "Performance Tests of a Fast-Acting Valve for the Driver Tubes of a Large Blast/Thermal Simulator." BRL-CR-687, U.S. Army Ballistic Research Laboratory, Aberdeen Proving Ground, MD, May 1992.

Szema, K. Y., S. R. Chakravarthy, D. Pan, and B. L. Bihari. "The Application of a Unified Marching Technique for flow over Complex 3-Dimensional Configurations Across the Mach Number Range." AIAA Paper No. 88-0276, 1988.

25

DISTRIBUTION LIST

No. of Copies	Organization
1	Director of Defense Research & Engineering ATTN: DD/TWP Washington, DC 20301
1	Assistant Secretary of Defense (Atomic Energy) ATTN: Document Control Washington, DC 20301
1	Chairman Joint Chiefs of Staff ATTN: J-5, R&D Division Washington, DC 20301
1	Deputy Chief of Staff for Operations and Plans ATTN: Technical Library Department of the Army Washington, DC 20310
1	European Research Office USARDSG (UK) ATTN: Dr. R. Reichenbach Box 65 FPO New York 09510-1500
1	Director Defense Advanced Research Projects Agency ATTN: Technical Library 3701 North Fairfax Drive Arlington, VA 22203-1714
1	Director Defense Intelligence Agency ATTN: DT-2/Wpns & Sys Div Washington, DC 20301
1	Director National Security Agency ATTN: R15, E. F. Butala Ft. George G. Meade, MD 20755

No. of Copies	Organization
7	Director Defense Nuclear Agency ATTN: CSTI, Technical Library DDIR DFSP NANS OPNA SPSD SPTD Washington, DC 20305
3	Commander Field Command, DNA ATTN: FCPR FCTMOF NMHE Kirtland AFB, NM 87115
10	Central Intelligence Agency DIR/DB/Standard ATTN: GE-47 HQ (10 cps) Washington, DC 20505
2	Commander, USACECOM ATTN: AMSEL-RD AMSEL-RO-TPPO-P Fort Monmouth, NJ 07703-5301
1	Commander, USACECOM R&D Technical Library ATTN: ASQNC-ELC-IS-L-R, Myer Center Fort Monmouth, NJ 07703-5000
1	Commander US Army Foreign Science and Technology Center ATTN: Research & Data Branch 220 7th Street , NE Charlottesville, VA 22901-5396
2	Commander US Army Strategic Defense Command ATTN: CSSD-H-MPL, Tech Lib CSSD-H-XM, Dr. Davies P.O. Box 1500 Huntsville, AL 35807

DISTRIBUTION LIST

No. of Copies	Organization

3	Commander
	US Army Corps of Engineers
	Waterways Experiment Station
	ATTN: CEWES-SS-R, J. Watt
	  CEWES-SE-R, J. Ingram
	  CEWES-TL, Tech Lib
	P.O. Box 631
	Vicksburg, MS 39180-0631

1	Commander US Army Research Office ATTN: SLCRO-D P.O. Box 12211 Research Triangle Park, NC 27709-2211
1	Commander US Army Test & Evaluation Command Nuclear Effects Laboratory ATTN: STEWS-TE-NO, Dr. J. L. Meason P.O. Box 477 White Sands Missile Range, NM 88002
2	Chief of Naval Operations Department of the Navy ATTN: OP-03EG OP-985F Washington, DC 20350
2	Office of Naval Research ATTN: Dr. A. Faulstick, Code 23 (2cps) 800 N. Quincy Street Arlington, VA 22217
1	Officer-in-Charge (Code L31) Civil Engineering Laboratory Naval Construction Battalion Center ATTN: Technical Library Port Hueneme, CA 93041
1	Commander Dahlgren Division Naval Surface Warfare Center ATTN: Code E23, Library Dahlgren, VA 22448-5000
1	Commander David Taylor Research Center ATTN: Code 522, Tech Info Ctr Bethesda, MD 20084-5000

No. of Copies	Organization
1	Officer in Charge White Oak Warfare Center Detachment ATTN: Code E232, Technical Library 10901 New Hampshire Avenue Silver Spring, MD 20903-5000
1	Commanding Officer White Oak Warfare Center ATTN: Code WA501, NNPO Silver Spring, MD 20902-5000
1	Commander (Code 533) Naval Weapons Center ATTN: Technical Library China Lake, CA 93555-6001
1	Commander Naval Weapons Evaluation Fac ATTN: Document Control Kirtland AFB, NM 87117
1	Commander Naval Research Laboratory ATTN: Code 2027, Technical Library Washington, DC 20375
1	AEDC ATTN: R. McAmis, Mail Stop 980 Arnold AFB, TN 37389
1	OLAC PL/TSTL ATTN: D. Shiplett Edwards AFB, CA 93523-5000
2	Air Force Armament Laboratory ATTN: AFATL/DOIL AFATL/DLYV Eglin AFB, FL 32542-5000
1	Phillips Laboratory (AFWL) ATTN: NTE Kirtland AFB, NM 87117-6008
1	AFIT ATTN: Technical Library, Bldg. 640/B Wright-Patterson AFB, OH 45433

DISTRIBUTION LIST

DISTRIBUTION LIST

No. of
Copies   Organization

1   MDA Engineering, Inc.
    ATTN: Dr. D. Anderson
    500 East Border Street
    Suite 401
    Arlington, TX 76010

1   Orlando Technology, Inc.
    ATTN: D. Matuska
    60 Second Street, Bldg. 5
    Shalimar, FL 32579

1   Science Applications International
        Corporation
    ATTN: J. Guest
    2301 Yale Blvd. SE, Suite E
    Albuquerque, NM 87106

2   Science Center
    Rockwell International Corporation
    ATTN: Dr. S. Chakravarthy
            Dr. D. Ota
    1049 Camino Dos Rios
    P. O. Box 1085
    Thousand Oaks, CA 91358

1   Sparta, Inc.
    Los Angeles Operations
    ATTN: I. B. Osofsky
    3440 Carson Street
    Torrance, CA 90503

1   S-CUBED
    A Division of Maxwell Laboratories, Inc.
    ATTN: Technical Library
    PO Box 1620
    La Jolla, CA 92037-1620

1   Sverdrup Technology, Inc.
    Sverdrup Corporation - AEDC
    ATTN: B. D. Heikkinen
    MS-900
    Arnold Air Force Base, TN 37389-9998

1   Battelle
    ATTN: TACTEC Library, J. N. Higgins
    505 King Avenue
    Columbus, OH 43201-2693

No. of
Copies   Organization

1   California Institute of Technology
    ATTN: T. J. Ahrens
    1201 E. California Blvd.
    Pasadena, CA 91109

2   Denver Research Institute
    ATTN: J. Wisotski
            Technical Library
    P.O. Box 10758
    Denver, CO 80210

1   Massachusetts Institute of Technology
    ATTN: Technical Library
    Cambridge, MA 02139

1   University of Minnesota
    AHPCRC
    ATTN: Dr. Tayfun E. Tezduyar
    1100 Washington Ave. South
    Minneapolis, Minnesota 55415

2   University of New Mexico
    New Mexico Engineering Research Institute
        (CERF)
    ATTN: Dr. J. Leigh
            Dr. R. Newell
    P.O. Box 25
    Albuquerque, NM 87131

1   Southwest Research Institute
    ATTN: Dr. C. Anderson
    P.O. Drawer 28255
    San Antonio, TX 78228-0255

1   State University of New York
    Mechanical & Aerospace Engineering
    ATTN: Dr. Peyman Givi
    Buffalo, NY 14260

Aberdeen Proving Ground

1   Cdr, USATECOM
    ATTN: AMSTE-TE-F, L. Teletski
1   Cdr, USATHMA
    ATTN: AMXTH-TE
1   Cdr, USACSTA
    ATTN: STECS-LI

29

USER EVALUATION SHEET/CHANGE OF ADDRESS

This Laboratory undertakes a continuing effort to improve the quality of the reports it publishes. Your comments/answers to the items/questions below will aid us in our efforts.

1. ARL Report Number _____ARL-TR-111_____ Date of Report ____April 1993____

2. Date Report Received _____

3. Does this report satisfy a need? (Comment on purpose, related project, or other area of interest for which the report will be used.) _____

_____

_____

4. Specifically, how is the report being used? (Information source, design data, procedure, source of ideas, etc.)_____

_____

_____

5. Has the information in this report led to any quantitative savings as far as man-hours or dollars saved, operating costs avoided, or efficiencies achieved, etc? If so, please elaborate. _____

_____

_____

6. General Comments. What do you think should be changed to improve future reports? (Indicate changes to organization, technical content, format, etc.) _____

_____

_____

_____

CURRENT
ADDRESS

Organization

Name

Street or P.O. Box No.

City, State, Zip Code

7. If indicating a Change of Address or Address Correction, please provide the Current or Correct address above and the Old or Incorrect address below.

OLD
ADDRESS

Organization

Name

Street or P.O. Box No.

City, State, Zip Code

(Remove this sheet, fold as indicated, tape closed, and mail.)
(DO NOT STAPLE)

DEPARTMENT OF THE ARMY

OFFICIAL BUSINESS

| | | | | | |

BUSINESS REPLY MAIL
FIRST CLASS PERMIT No 0001, APG, MD

Postage will be paid by addressee.

Director
U.S. Army Research Laboratory
ATTN: AMSRL-OP-CI-B (Tech Lib)
Aberdeen Proving Ground, MD 21005-5066